

Testing the Cosmological Principle in the radio sky

Carlos A. P. Bengaly,^a Roy Maartens,^{a,b} Nandrianina
Randriamiarinarivo,^a Albert Baloyi^a

^aDepartment of Physics & Astronomy, University of the Western Cape,
Cape Town 7535, South Africa

^bInstitute of Cosmology & Gravitation, University of Portsmouth,
Portsmouth PO1 3FX, United Kingdom

E-mail: carlosap87@gmail.com, roy.maartens@gmail.com,
nandrianiana@gmail.com, mathobela.baloyi@gmail.com

Abstract. The Cosmological Principle states that the Universe is statistically isotropic and homogeneous on large scales. In particular, this implies statistical isotropy in the galaxy distribution, after removal of a dipole anisotropy due to the observer's motion. We test this hypothesis with number count maps from the NVSS radio catalogue. We use a local variance estimator based on patches of different angular radii across the sky and compare the source count variance between and within these patches. In order to assess the statistical significance of our results, we simulate radio maps with the NVSS specifications and mask. We conclude that the NVSS data is consistent with statistical isotropy.

Contents

1	Introduction	1
2	Data and simulations	2
3	Probing isotropy	3
4	Results	5
5	Conclusions	6

1 Introduction

The standard Λ CDM model provides the best current framework consistent with observations of the cosmic microwave background (CMB) and of the large-scale structure of the matter distribution (e.g. [1, 2]). One of the most fundamental pillars of the standard model is the Cosmological Principle, i.e., the hypothesis that the Universe follows statistical homogeneity and isotropy on large scales. Testing these assumptions in light of observational data is an essential robustness check of the standard cosmological model. (Note that dynamical dark energy models and modified gravity models also rely on the Cosmological Principle.)

Statistical homogeneity is more challenging to test than statistical isotropy – since observations can directly probe isotropy (on the observer’s past lightcone), whereas spatial variations on cosmological scales (inside the observer’s past lightcone) cannot be directly measured. Here we focus on direct tests of isotropy.

The CMB delivers the most precise tests of isotropy, with its all-sky coverage and exquisite data. It is isotropic at a $\sim 10^{-5}$ level, after the $\sim 10^{-3}$ dipole, due to our motion relative to the CMB frame, is removed. However, near-isotropy of the CMB does *not* in itself imply near-isotropy of the Universe [3]. We also need independent probes of anisotropy in the matter distribution. These probes constitute a critical consistency test of statistical isotropy.

Previous work has shown no statistically significant violation of isotropy in the observational data of Type Ia Supernova distances [4, 5, 6] and of gamma-ray bursts [7, 8, 9]. More stringent tests require the far higher number densities delivered by large galaxy surveys. The simplest way to test consistency with the CMB is to measure the dipole of a (sufficiently wide) galaxy survey, which should be aligned with the direction of the CMB dipole [10, 11, 12, 13, 14, 15, 16, 17, 18, 19, 20, 21, 22]. For currently available data sets, the matter dipole direction is not inconsistent with the CMB, but the amplitude is too large, probably arising from the quality of current data sets. Forecasts predict that future all-sky radio continuum surveys with the SKA should achieve the accuracy necessary to make a stringent test of consistency with the CMB dipole [23, 24].

Measuring the dipole is sufficient to reveal a possible inconsistency on the largest scales, but this test is not possible for most surveys of the matter distribution since they are not wide enough. Furthermore, in order to systematically test isotropy, as opposed to a consistency test, we need to probe smaller scales. On smaller scales than the dipole, some isotropy tests have

been performed on galaxy surveys, including infrared [25], optical [26] and radio [27, 28, 29, 30] surveys. The results so far are consistent with isotropy.

In this paper, we analyse the number counts of the widest galaxy survey, the NRAO VLA Sky Survey (NVSS). The wide area of NVSS allows us to use a high number of sky patches for testing isotropy, increasing the statistical power of the test. In our test, we use an estimator not previously applied to galaxy surveys. In order to assess the statistical significance of our analysis, we produce mock data sets, using the Λ CDM background to generate an angular power spectrum, and using the results of simulations to estimate the clustering properties of radio sources. A log-normal code is then applied to the angular power spectrum to generate mock sky maps.

The paper is organised as follows: section 2 describes the observational and simulated data; section 3 discusses our estimator; section 4 presents the results and, finally, our discussion and concluding remarks are given in section 5.

2 Data and simulations

The data we use is from the NVSS radio continuum survey at 1.4 GHz [31]. The NVSS catalogue covers all the northern sky, as well as most of the southern sky except for the lowest declinations, that is, $\text{DEC} < 40^\circ$. In our analysis, we choose a flux density range following [21]:

$$20 \text{ mJy} < S < 1000 \text{ mJy} . \quad (2.1)$$

This is a conservative choice in order to ensure sample completeness (lower limit) and elimination of very bright sources (upper limit). Since the NVSS flux densities are found to be statistically isotropic in the sky [30], no further flux cutoff is performed.

We construct a mask which excises the following regions, as in [21]:

- Close to the galactic plane, i.e., $|b| \leq 10^\circ$.
- Within 1° of the local radio sources and local superclusters (see also [19]).
- Galactic foreground emission above $T = 50 \text{ K}$ according to the 408 MHz continuum map in [32].

In addition, we follow [12, 30] and excise the region:

- Within a 5° degree radius around $(l, b) = (207.13^\circ, -17.84^\circ)$.

This region of anomalously high source counts could bias our results. We computed the rms flux density measurement errors in the region, finding that they are compatible with the errors of the whole NVSS sample. Hence only the source counts are anomalous, not the source properties.

The resulting sky coverage is $f_{\text{sky}} \simeq 0.657$ after producing a pixelised count map using HEALPIX [33]¹. Mock NVSS catalogues are produced as in [21]:

- Choose five redshift bins in $0 < z < 4$, with edges at $z = 0.0, 0.5, 1.0, 2.0, 3.0, 4.0$.
- Obtain the redshift distribution of radio sources from an SQL query over 121 deg^2 on the S^3 (SKA Simulated Skies) [34] website².

¹ <https://healpix.sourceforge.io/>

² http://s-cubed.physics.ox.ac.uk/s3_sex

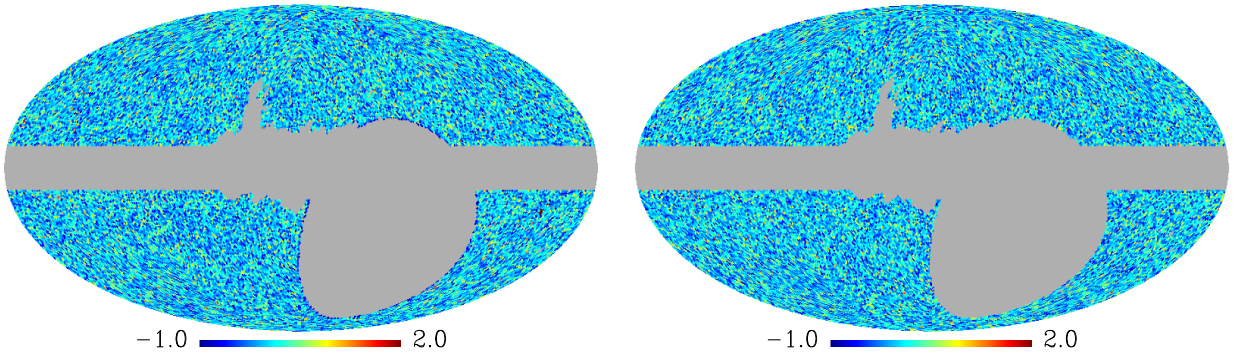


Figure 1. Real (left) and one example mock (right) NVSS maps of number density contrast $\delta_n = (n - \bar{n})/\bar{n}$, using the HEALPIX grid resolution $N_{\text{side}} = 64$.

- Model the redshift-dependent bias following [18]: $b(z) = 1.6 + 0.7z + 0.35z^2$.
- Compute the angular power spectrum using CAMB SOURCES [35] in each redshift bin, using the Planck 2015 Λ CDM best-fit parameters [36]. (Note that the Λ CDM best-fit power spectrum changes very little between Planck 2015 and 2018.)
- In each redshift bin, input the CAMB angular power spectrum into the FLASK code [37] to produce 1000 NVSS realisations, following a lognormal distribution for density fluctuations. Produce mock maps in each bin, stacking them afterwards to produce a full NVSS map covering $0 < z < 4$.

This prescription generates mock realisations that are statistically isotropic. Then we add to the mock counts a fiducial kinematic dipole signal, based on the measurement reported in [21] (see [23] for details). The pixelised count maps of the real data, and one of the NVSS realisations, are shown in Figure 1.

3 Probing isotropy

We perform a statistical isotropy test on the NVSS data according to the following prescription.

- We define 3072 directions in the sky coinciding with the $N_{\text{side}} = 16$ pixel centres.
- Around each centre, we draw a patch of angular radius θ , where

$$\text{angular size of patches: } \theta = 15^\circ, 20^\circ, 25^\circ \text{ and } 30^\circ. \quad (3.1)$$

- When a patch overlaps the masked sky area, we need to decide a threshold of masking in the patch, above which the patch should be rejected for the test (see also [25, 38]). If m is the threshold percentage of masked pixels in a patch, then we reject the patch if its percentage of masked pixels is $> m$. We choose

$$\text{threshold of masked pixels in patch: } m = 10\%, 30\% \text{ and } 50\%, \quad (3.2)$$

i.e., from strict to weak rejection criteria. Note that our criteria is stricter than those assumed in [25, 38], which used $m = 90\%$, in order to avoid further biases due to incomplete sky coverage.

A patch p has μ_p pixels, with n_{pi} radio sources in pixel i . The total number of sources in the patch is $n_p = \sum_i n_{pi}$, and the average number per pixel is $\bar{n}_p = n_p/\mu_p$. Then the variance in the patch p is

$$\sigma_p^2 = \frac{1}{(\mu_p - 1)} \sum_{i=1}^{\mu_p} (n_{pi} - \bar{n}_p)^2. \quad (3.3)$$

We assess the level of statistical isotropy of the NVSS sample in different patches by means of the Anova (Analysis of Variance) approach [39], which is a collection of methods to compare multiple means. We use it to produce a comparison of the mean number counts between the patches, and also within each patch.

Like most statistical tests, we accept or reject the null hypothesis of a certain feature of the data. Anova uses the F -ratio to provide a quantity that measures the differences amongst all of the mean counts in patches [39]. It is defined as:

$$F = \frac{\text{variance between patches}}{\text{variance within patches}}. \quad (3.4)$$

Then we have

$$\text{exactly isotropic data:} \quad F = 1. \quad (3.5)$$

Since the real and mock counts are generated by gravitational clustering, we expect some deviation from 1 even for statistically isotropic data.

We need to define a criterion by which we accept or reject the null hypothesis, that is, that the Universe is not statistically isotropic. We use the 5th and 95th percentiles of the F -distribution as the upper limit of statistical isotropy – noting that the mock realisations are statistically isotropic by construction. If the F -value of the real data disagrees with that, it would be an indication of statistical isotropy violation. If not, we reject the null hypothesis.

In addition to the Anova test, we use another method to assess the statistical isotropy of the NVSS data. It is based on the Local Variance (LV) estimator defined in [38] (see also [25]), and it provides a more direct method to visualise the deviation of the mean counts per patch across the sky between the real and the mock data. The LV estimator is defined for each patch as

$$\text{LV}_p = \frac{(\sigma_p/M)_{\text{data}} - (\overline{\sigma_p/M})_{\text{mock}}}{(\sigma_p/M)_{\text{mock}}}, \quad (3.6)$$

where σ_p is given by (3.3) and M is the average source count per patch. This is given by $M = \sum_p n_p/N$, where N is the number of accepted patches. We compare the coefficient of variation in every patch drawn in the real data map, $(\sigma_p/M)_{\text{data}}$, with the average coefficient of variation per patch over all mock realisations, $(\overline{\sigma_p/M})_{\text{mock}}$.

Note that the LV estimator only provides visual information of the variance fluctuation across the sky, which is why we deploy the F -ratio and F -distribution as a metric to quantify how consistent with the statistical isotropy assumption the NVSS data is.

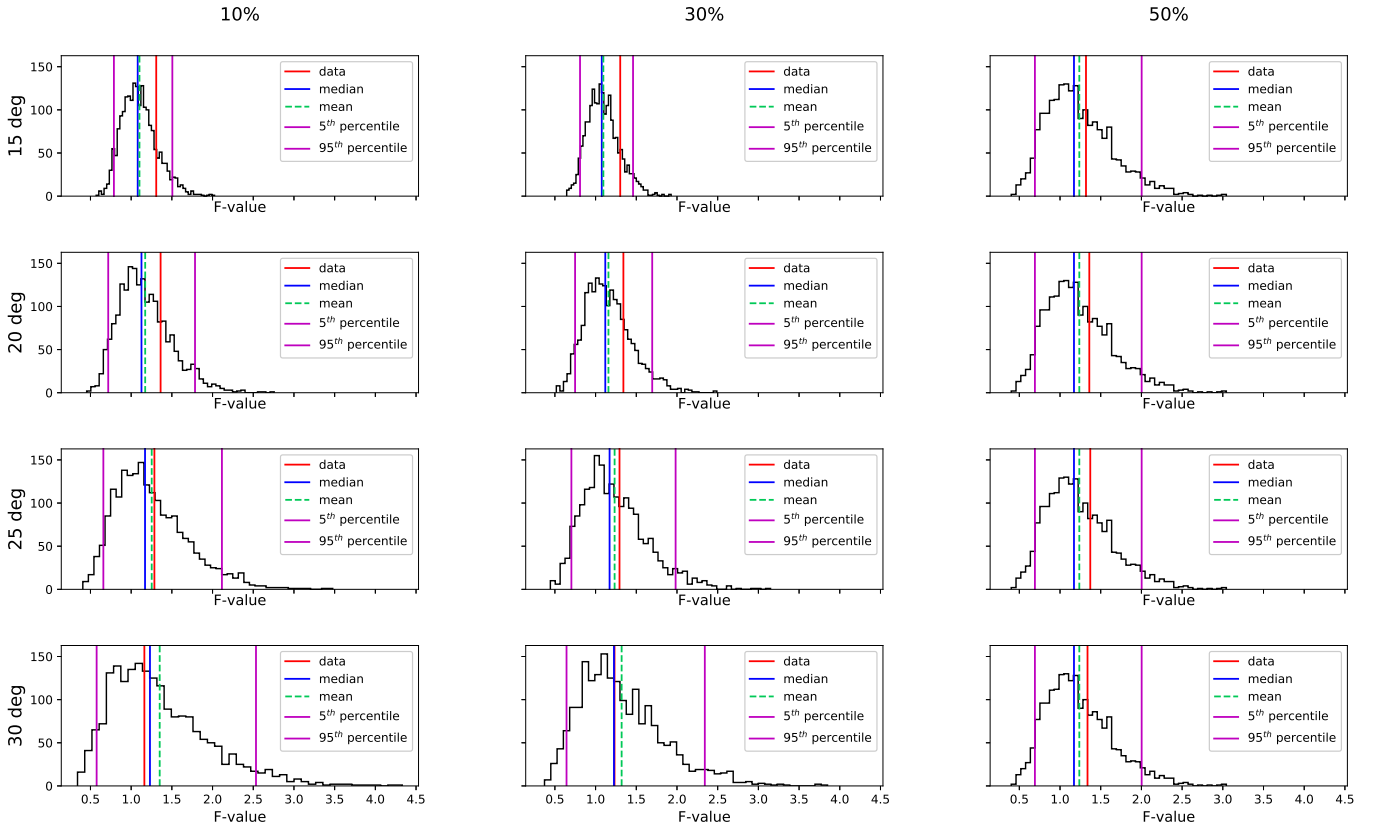


Figure 2. F -distribution of the NVSS realisations (black histogram) and F -value of the NVSS data (red vertical line), for 4 patch radii (rows) and 3 masked pixel rejection thresholds (columns). Also shown are: 5th and 95th percentiles (magenta), the mean (dashed green) and the median (blue) of the F -distribution.

4 Results

We show the F -distribution of the mock realisations as compared to the real NVSS data in Figure 2. All the distributions peak around 1. Vertical lines indicate the 5th and 95th percentiles, the mean and the median of the F -distribution, together with the F -statistic of the real data.

The F -distribution exhibits a larger tail-end at $F > 1$ as we increase the patch radius. This is an expected feature, since the shape of the distribution depends on the degrees of freedom, and we have a smaller number of accepted patches for larger patches.

We note that the F -value obtained from the real data is in excellent agreement with both the mean and the median F -values of the mock realisations, regardless of the patch radius size and the rejection criterion adopted. They are all close to the vertical line around 1, and well within the 5th and 95th boundaries obtained from the simulations.

Statistical isotropy of the source counts is also evident in the local variance maps shown in Figure 3: there is no indication of preferred directions, or anomalous variance, across the sky.

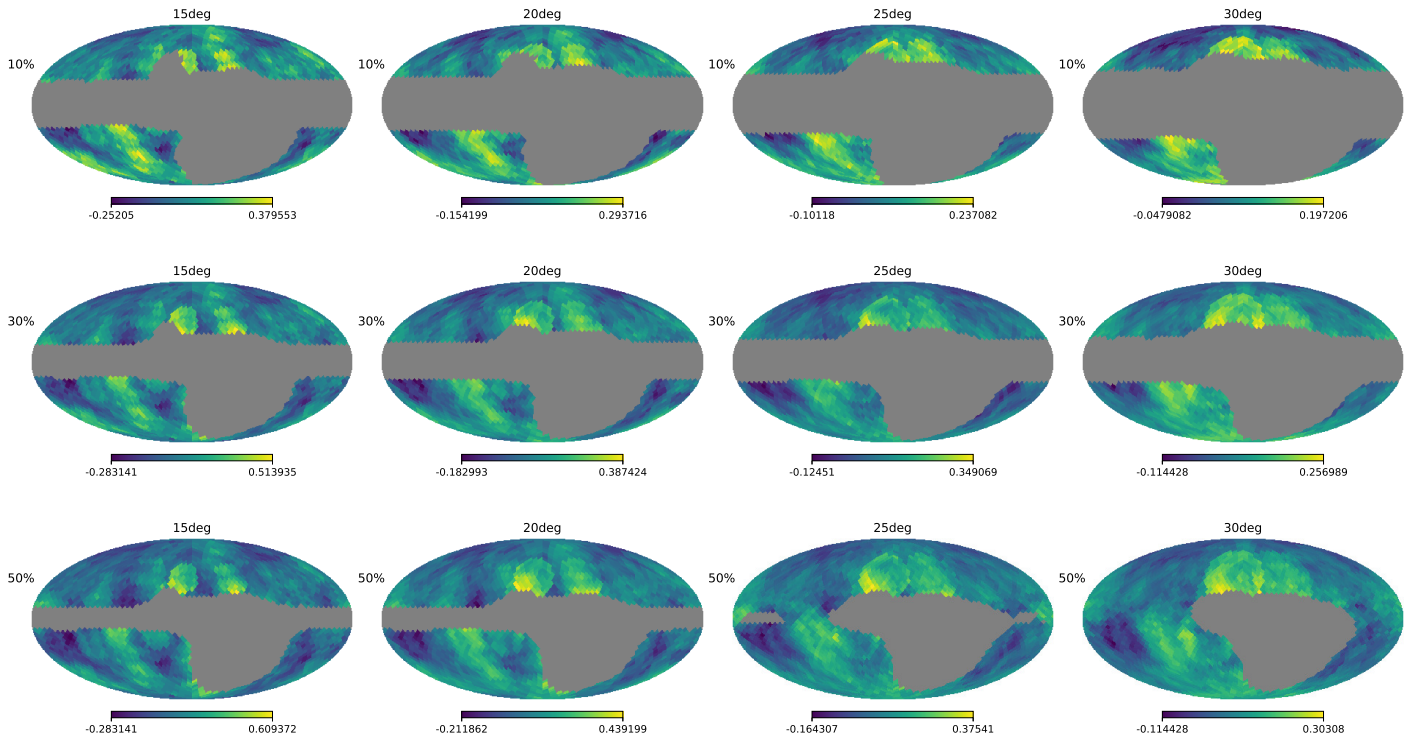


Figure 3. Map of local variance (3.6), for 4 patch radii (columns) and 3 masked pixel rejection thresholds (rows).

Thus, on the basis of the F and local variance tests, we can safely reject the null hypothesis – that the Universe is not statistically isotropic – and conclude that the NVSS catalogue is indeed statistically isotropic at $15^\circ - 30^\circ$ angular scales.

5 Conclusions

In this work, we tested whether the NVSS catalogue is consistent with the statistical isotropy hypothesis on angular scales smaller than the dipole – whose amplitude is known to be larger than expected. We constructed a mask that extends the mask in [21] by excising a small region of anomalously high source counts, following [12, 30]. We simulated radio sky maps that reproduce the NVSS specifications, as well as the radio source clustering and the power spectrum of the standard model, following [21]. A dipole modulation consistent with the kinematic dipole signal observed in the real data was also applied in these mocks [21, 23].

Our test consists of drawing patches across the sky with different angular radii, (3.1), and different rejection thresholds to eliminate masked pixels within the patches, (3.2). We apply an LV estimator, in addition to the AnoVa test, to compare the data with the simulations. This AnoVa test provides us with an F -value for the real data, and a distribution of F -values for the mock realisations, as a metric that quantifies how consistent are these patches across the sky. In other words, it quantifies how isotropic these source count maps are. Because the mocks are statistically isotropic by construction, they constitute a benchmark for isotropy. Hence, our null hypothesis is that the real data is not consistent with the mocks – i.e., that

the NVSS is not consistent with statistical isotropy – within the 5th–95th percentile region of the F -distribution.

We found that the observed radio counts reject the null hypothesis, since the data agrees with the mock maps produced for patches of all chosen radii and with all masked pixel rejection thresholds. As we increase the patch radius, the discrepancy between the data and simulations becomes smaller, since we encompass a larger number of sources so that the shot noise is reduced. In addition, we noticed that the more rigorous we were in the rejection of masked pixels, the better is the agreement between the real data and statistically isotropic realisations. We found an optimum choice for patch radius of 25° and for rejection threshold of 30%.

Therefore, there is no signal of isotropy violation in the NVSS source counts on smaller angular scales than the dipole. This result agrees with the findings of [28, 29, 30], using other methods of analysis. A more thorough investigation of the impact of clustering bias models (which can affect the large angular scales), as well as of magnification bias and redshift distribution modelling of the source counts, is left for future work.

Finally, we stress that our method is completely general, and can be readily applied to larger and more complete data sets from next-generation surveys, such as forthcoming radio continuum surveys with the SKA precursor survey EMU [40] and with SKA Phase 1 [41], and future redshift surveys with SKA1 [41], J-PAS [42], LSST [43] and Euclid [44].

Acknowledgements:

We thank Matt Jarvis and Mario Santos for useful discussions. This work was supported by the South African SKA Project and the National Research Foundation of South Africa (Grant No. 75415). RM was also supported by the UK STFC (Grant ST/S000550/1). Some of our results made use of the HEALPIX package [33].

References

- [1] N. Aghanim *et al.* [Planck Collaboration], “Planck 2018 results. VI. Cosmological parameters,” [arXiv:1807.06209].
- [2] G. B. Zhao *et al.*, “The clustering of the SDSS-IV extended Baryon Oscillation Spectroscopic Survey DR14 quasar sample: a tomographic measurement of cosmic structure growth and expansion rate based on optimal redshift weights,” *Mon. Not. Roy. Astron. Soc.* **482**,3497 (2019) [arXiv:1801.03043].
- [3] C. Clarkson and R. Maartens, “Inhomogeneity and the foundations of concordance cosmology,” *Class. Quant. Grav.* **27**, 124008 (2010) [arXiv:1005.2165].
- [4] D. Huterer, D. Shafer, D. Scolnic and F. Schmidt, “Testing Λ CDM at the lowest redshifts with SN Ia and galaxy velocities,” *JCAP* **1705**, 015 (2017) [arXiv:1611.09862].
- [5] U. Andrade, C. A. P. Bengaly, B. Santos and J. S. Alcaniz, “A Model-independent Test of Cosmic Isotropy with Low- z Pantheon Supernovae,” *Astrophys. J.* **865**, 119 (2018) [arXiv:1806.06990].
- [6] J. Soltis, A. Farahi, D. Huterer and C. M. Liberato, “Percent-Level Test of Isotropic Expansion Using Type Ia Supernovae,” *Phys. Rev. Lett.* **122**, 091301 (2019) [arXiv:1902.07189].
- [7] T. N. Ukwatta and P. R. Wozniak, “Investigation of Redshift- and Duration-Dependent Clustering of Gamma-ray Bursts,” *Mon. Not. Roy. Astron. Soc.* **455**, 703 (2016) [arXiv:1507.07117].
- [8] J. Ripa and A. Shafieloo, “Testing the Isotropic Universe Using the Gamma-Ray Burst Data of Fermi/GBM,” *Astrophys. J.* **851**, 15 (2017) [arXiv:1706.03556].
- [9] U. Andrade, C. A. P. Bengaly, J. S. Alcaniz and S. Capozziello, “Revisiting the statistical isotropy of GRB sky distribution,” [arXiv:1905.0886]
- [10] G. F. R. Ellis and J. E. Baldwin, “On the expected anisotropy of radio source counts," *Mon. Not. Roy. Astron. Soc.* **206**, 377 (1984).
- [11] A. Baleisis, O. Lahav, A. J. Loan and J. V. Wall, “Searching for large scale structure in deep radio surveys,” *Mon. Not. Roy. Astron. Soc.* **297**, 545 (1998) [astro-ph/9709205].
- [12] C. Blake and J. Wall, “Detection of the velocity dipole in the radio galaxies of the NRAO VLA sky survey,” *Nature* **416**, 150 (2002) [astro-ph/0203385].
- [13] F. Crawford, “Detecting the Cosmic Dipole Anisotropy in Large-Scale Radio Surveys,” *Astrophys. J.* **692**, 887 (2009) [arXiv:0810.4520].
- [14] Y. Itoh, K. Yahata and M. Takada, “A dipole anisotropy of galaxy distribution: Does the CMB rest-frame exist in the local universe?,” *Phys. Rev. D* **82**, 043530 (2010) [arXiv:0912.1460].
- [15] A. K. Singal, “Large peculiar motion of the solar system from the dipole anisotropy in sky brightness due to distant radio sources,” *Astrophys. J.* **742**, L23 (2011) [arXiv:1110.6260].
- [16] C. Gibelyou and D. Huterer, “Dipoles in the Sky,” *Mon. Not. Roy. Astron. Soc.* **427**, 1994 (2012) [arXiv:1205.6476].

- [17] M. Rubart and D. J. Schwarz, “Cosmic radio dipole from NVSS and WENSS,” *Astron. Astrophys.* **555**, A117 (2013) [arXiv:1301.5559].
- [18] P. Tiwari and A. Nusser, “Revisiting the NVSS number count dipole,” *JCAP* **1603**, 062 (2016) [arXiv:1509.02532].
- [19] J. Colin, R. Mohayaee, M. Rameez and S. Sarkar, “High redshift radio galaxies and divergence from the CMB dipole,” *Mon. Not. Roy. Astron. Soc.* **471**, 1045 (2017) [arXiv:1703.09376].
- [20] R. Maartens, C. Clarkson and S. Chen, “The kinematic dipole in galaxy redshift surveys,” *JCAP* **1801**, 013 (2018) [arXiv:1709.04165].
- [21] C. A. P. Bengaly, R. Maartens and M. G. Santos, “Probing the Cosmological Principle in the counts of radio galaxies at different frequencies,” *JCAP* **1804**, 031 (2018) [arXiv:1710.08804].
- [22] A. K. Singal, “A large disparity in cosmic reference frames determined from the sky distributions of radio sources and the microwave background radiation,” arXiv:1904.11362.
- [23] C. A. P. Bengaly, T. M. Siewert, D. J. Schwarz and R. Maartens, “Testing the standard model of cosmology with the SKA: the cosmic radio dipole,” *Mon. Not. Roy. Astron. Soc.* **486**, 1350 (2019) [arXiv:1810.04960].
- [24] N. Pant, A. Rotti, C. A. P. Bengaly and R. Maartens, “Measuring our velocity from fluctuations in number counts,” *JCAP* **1903**, 023 (2019) [arXiv:1808.09743].
- [25] D. Alonso, A. I. Salvador, F. J. Sánchez, M. Bilicki, J. Garcia-Bellido and E. Sánchez, “Homogeneity and isotropy in the Two Micron All Sky Survey Photometric Redshift catalogue,” *Mon. Not. Roy. Astron. Soc.* **449**, 670 (2015) [arXiv:1412.5151].
- [26] S. Sarkar, B. Pandey and R. Khatri, “Testing isotropy in the Universe using photometric and spectroscopic data from the SDSS,” *Mon. Not. Roy. Astron. Soc.* **483**, 2453 (2019) [arXiv:1810.07410].
- [27] S. Rana and J. S. Bagla, “Angular clustering of point sources at 150 MHz in the TGSS survey,” *Mon. Not. Roy. Astron. Soc.* **485**, 5891 (2019) [arXiv:1802.05001].
- [28] P. Tiwari and P. K. Aluri, “Large Angular-scale Multipoles at Redshift 0.8,” *Astrophys. J.* **878**, 32 (2019) [arXiv:1812.04739].
- [29] A. Dolfi, E. Branchini, M. Bilicki, A. Balaguera-Antolínez, I. Prandoni and R. Pandit, “Clustering properties of TGSS radio sources,” *Astron. Astrophys.* **623**, A148 (2019) [arXiv:1901.08357].
- [30] P. Tiwari, S. Ghosh and P. Jain, “The galaxy power spectrum from TGSS ADR1 and the effect of flux calibration systematics,” arXiv:1907.10305.
- [31] J. J. Condon, W. D. Cotton, E. W. Greisen, Q. F. Yin, R. A. Perley, G. B. Taylor and J. J. Broderick, “The NRAO VLA Sky Survey,” *Astron. J.* **115**, 1693 (1998).
- [32] C. G. T. Haslam, C. J. Salter, H. Stoffel and W. E. Wilson, “A 408 MHz all-sky continuum survey. II. The atlas of contour maps,” *Astron. Astrophys. Suppl. Ser.* **47**, 1 (1982).
- [33] K. M. Gorski, E. Hivon, A. J. Banday, B. D. Wandelt, F. K. Hansen, M. Reinecke and M. Bartelman, “HEALPix - A Framework for high resolution discretization, and fast analysis of data distributed on the sphere,” *Astrophys. J.* **622**, 759 (2005) [astro-ph/0409513].
- [34] R. J. Wilman *et al.*, “A semi-empirical simulation of the extragalactic radio continuum sky for next generation radio telescopes,” *Mon. Not. Roy. Astron. Soc.* **388**, 1335 (2008) [arXiv:0805.3413].
- [35] A. Challinor and A. Lewis, “The linear power spectrum of observed source number counts,” *Phys. Rev. D* **84**, 043516 (2011) [arXiv:1105.5292].
- [36] P. A. R. Ade *et al.* [Planck Collaboration], “Planck 2015 results. XIII. Cosmological parameters,” *Astron. Astrophys.* **594**, A13 (2016) [arXiv:1502.01589].

- [37] H. S. Xavier, F. B. Abdalla and B. Joachimi, “Improving lognormal models for cosmological fields,” *Mon. Not. Roy. Astron. Soc.* **459**, 3693 (2016) [arXiv:1602.08503].
- [38] Y. Akrami, Y. Fantaye, A. Shafieloo, H. K. Eriksen, F. K. Hansen, A. J. Banday and K. M. Górski, “Power asymmetry in WMAP and Planck temperature sky maps as measured by a local variance estimator,” *Astrophys. J.* **784**, L42 (2014) [arXiv:1402.0870].
- [39] F. J. Gravetter, *Statistics for the behavioral sciences*, Wadsworth Publishing, 9 ed. (2012).
- [40] R. P. Norris *et al.*, “EMU: Evolutionary Map of the Universe,” *Publ. Astron. Soc. Austral.* **28**, 215 (2011) [arXiv:1106.3219].
- [41] D. J. Bacon *et al.* [SKA Collaboration], “Cosmology with Phase 1 of the Square Kilometre Array: Red Book 2018: Technical specifications and performance forecasts,” arXiv:1811.02743.
- [42] N. Benitez *et al.* [J-PAS Collaboration], “J-PAS: The Javalambre-Physics of the Accelerated Universe Astrophysical Survey,” arXiv:1403.5237.
- [43] P. A. Abell *et al.* [LSST Collaboration], “LSST Science Book, Version 2.0,” arXiv:0912.0201.
- [44] L. Amendola *et al.*, “Cosmology and fundamental physics with the Euclid satellite,” *Living Rev. Rel.* **21**, 2 (2018) [arXiv:1606.00180].